Appendix A: Analytical methods

A.1 XRD

Soils were micronized and characterized at Trent University using a Bruker D2 Phaser diffractometer equipped with a LYNXEYE XE-T position-sensitive detector coupled with a 0.6 mm divergence slit and incident and diffracted beam Soller slits. Micronized samples were prepared as powder mounts in back-loading holders. A fine-focus Cu X-ray tube using a 6º take-off angle was operated at 30 kV and 10 mA for X-ray generation in the diffractometer. Qualitative patterns were collected over a 2θ range of 5–80° with a step size of 0.02°/step at a rate of 4 s/step with a 15-rpm spin. Mineral phase identification from XRD scans was conducted using the DIFFRAC.EVA Version 5 XRD phase analysis software (Bruker) with reference to the International Center for Diffraction Data Powder Diffraction File 2 2020 database (ICDD PDF2). Quantitative analysis was conducted using TOPAS Version 6 software (Bruker) to provide weight-percent (wt.%) values to the pattern phases.

A.2 XRF

X-ray fluorescence (XRF) spectroscopy was conducted at SGS Minerals, Burnaby, British Columbia, Canada, on micronized samples to determine bulk geochemical compositions of the kimberlite, soil, and mixtures. The trace element composition was determined by digesting samples with four acids (nitric, hydrofluoric, perchloric and hydrochloric acid), ensuring dissolution of silicate minerals present, and analyzing trace elements by inductively coupled plasma-optical emission spectroscopy (ICP-OES). Detection limits for all oxides was 0.01 wt.% and Detection limits of 1 ppm for Ni and Cr.

A.3 CEC

Cation exchange capacity (CEC) of samples (10 g) were expressed in milli-equivalents per 100 g of dry sample (meq/100 g) or centi-moles of charge per kg (cmol/kg). Samples were saturated with a buffered 1.0 M ammonium acetate (NH_4^+-Ac) solution then leached with an un-buffered 1.0 M potassium chloride (KCl) solution. Analysis of exchangeable cations (Na, K, Ca, and Mg) is achieved by analyzing the NH_4^+ saturated leachate prior to KCl leaching. Total CEC is calculated from NH_4^+-N concentration analysed in the KCl leachate via colorimetry.

A.4 SSA

A nitrogen gas (N_2) adsorption method was used to determine the Brunauer–Emmett–Teller (BET) specific surface areas (Brunauer et al., 1938). Untreated samples were degassed overnight using a Smart VacPrepTM 067 (Micromeritics, Norcross, GA, USA), with samples kept at a temperature of 200 ºC for 10 h. Analysis was performed at 77 K (-196 ºC) on the Micromeritics TriStar II Plus adsorption unit (Micromeritics, Norcross, GA, USA), and N_2 isotherms were acquired using a partial pressure range of 0.01–0.90. Treated sampled consisted of removing the organic matter from field experiment soils using a modified method by Feller et al. (1992). Samples were reacted with 50 mL of 30% H_2O_2 in 125 mL polycarbonate flasks and mixed on a shaker table (125 rpm) for 1 day. Sample slurries were poured into glass Petri dishes and left to dry, conducting BET analyses on these treated samples to determine the specific surface areas of the inorganic fraction. All data processing was conducted using MicroActive Interactive software (Micromeritics, Norcross, GA, USA).

A.5 PSD

Particle size distributions of solid samples were analyzed using a Horiba LA-950V2 laser scattering particle size distribution analyzer (Teledyne: USA) which is accurate within ±0.6%. Sodium hexametaphosphate (30 g/L) was used as a dispersant agent to prevent flocculation of samples. Duplicate samples were sonicated in three 1 min intervals using the Horiba system, with a standard of pulverized quartz sand analyzed as an in-house reference for assessing analytical error.

A.6 Geochemical modelling

PHREEQC (Parkhurst and Appelo, 2013), and the carbfix.dat database (Voigt et al., 2018), were used to determine saturation indices and equilibrium states of mineral phases. This thermodynamic modelling program applies water chemistry and mineralogical data to determine the mineral solubility, saturation, and speciation of specified minerals in each sample. Saturation indices were determined for calcite, forsterite, lizardite, phlogopite, and saponite with parameters set to corresponding pH values, a default temperature of 25 ºC, and a water volume of 1 L. Data points were acceptable if PHREEQC outputs consisted of charge balances within ±15%.

A.7 Alkalinity

Alkalinity analyses were conducted on water samples using a Xylem TitroLine® 7000-M2/20 titrator. The instrument was calibrated daily using blanks (ASTM Type II Deionized, Distilled water, Sigma-Aldrich Canada) and 500 and 100 ppm standards of $NaHCO_3$. Samples were diluted by a maximum dilution factor of 4 and mixed using a 2 cm stir bar in 30 mL beakers. Initial pH was measured using an SI Analytics® Blueline pH electrode which recorded

pH continuously for the analysis duration. After a 25 s hold, the system titrates 0.01 N HCl in 0.025 mL increments until an endpoint of pH 3.1 is reached. The equivalence volume was calculated using the Gran method where HCO_3^- concentrations were calculated from the generated intercept where all HCO_3^- had converted to H_2CO_3 (Gran, 1952).

Appendix B: Monthly percolation values

Table B.1. Monthly percolation values for Chapter 2 (control, K10+30, and K20 plot) and Chapter 3 (control, Ol10, Ol20). N/A indicates months that were unmonitored. ND indicates no data was collected due to probe malfunction.

	2021	2022	2023		2022	2023
January	N/A	N/A		**January**	N/A	
Control			13.2	Control		18.7
K10+30			ND	Ol10		26.3
K20			13.1	Ol20		20.7
February	N/A	N/A		**February**	N/A	
Control			13.3	Control		15.9
K10+30			32.0	Ol10		14.7
K20			17.5	Ol20		16.3
March	N/A	N/A		**March**	N/A	
Control			10.5	Control		17.9
K10+30			20.4	Ol10		2.2
K20			13.6	Ol20		18.4
April	N/A	N/A		**April**	N/A	
Control			35.1	Control		60.4
K10+30			44.6	Ol10		63.1
K20			45.9	Ol20		47.0
May	N/A			**May**		
Control		27.7	36.2	Control	11.2	42.7
K10+30		40.8	49.3	Ol10	18.3	37.1
K20		32.9	52.7	Ol20	10.5	47.1
June				**June**		
Control	15.9	39.7	22.1	Control	30.4	29.7
K10+30	23.5	53.7	22.4	Ol10	31.6	12.1
K20	17.3	50.5	25.5	Ol20	41.1	33.9
July				**July**		
Control	25.3	10.4	28.3	Control	23.5	27.3
K10+30	21.8	6.21	28.1	Ol10	30.7	14.9
K20	37.1	5.5	47.6	Ol20	23.0	45.1
August				**August**		
Control	49.8	7.59	35.1	Control	31.1	24.1
K10+30	50.4	22.7	39.4	Ol10	5.3	32.6
K20	25.5	0.06	37.4	Ol20	4.3	27.1
September				**September**		
Control	3.79	0.15	20.4	Control	1.5	ND
K10+30	21.7	13.5	11.1	Ol10	1.4	ND
K20	27.7	3.08	9.49	Ol20	1.7	ND
October			N/A	**October**		
Control	14.2	0.23		Control	3.4	4.1
K10+30	23.0	3.62		Ol10	2.2	4.3
K20	42.6	18.5		Ol20	3.6	4.1
November	N/A		N/A	**November**		
Control		4.12		Control	15.6	15.9
K10+30		0.09		Ol10	6.5	1.3
K20		2.53		Ol20	8.8	7.7
December	N/A		N/A	**December**		
Control		6.39		Control	6.8	42.7
K10+30		2.68		Ol10	12.9	37.1
K20		11.3		Ol20	10.0	47.1

Annual precipitation: 2021 (794 mm), 2022 (800 mm), 2023 (804 mm)

Appendix C: Saturation indices

Table C.1. Annual saturation indices of calcite, dolomite, forsterite, lizardite, saponite, hydromagnesite, and amorphous silica in the porewaters of the control, K10+30, and K20 plot. Values are an average over the monitoring period of at least 4 samples.

	Calcite	Dolomite	Forsterite	Lizardite	Saponite	Hydromagnesite	SiO_2 (am)
Control							
2021	0.66	0.50	-10.30	-6.41	-6.51	-16.80	-1.47
2022	0.80	0.68	-9.83	-5.66	-5.67	-16.45	-1.50
2023	0.77	0.67	-9.78	-5.69	N/A	-16.26	-1.59
K10+30							
2021	0.89	1.03	-9.48	-5.13	-5.09	-15.24	-1.40
2022	1.39	2.13	-6.13	0.14	0.96	-9.87	-1.02
2023	0.97	1.80	-7.61	-2.10	N/A	-11.76	-0.95
K20							
2021	1.02	1.37	-8.89	-4.16	-3.80	-14.17	-1.21
2022	1.11	1.80	-7.92	-2.62	-2.08	-12.40	-1.05
2023	0.83	1.39	-7.66	-2.20	N/A	-12.81	-0.98

Table C.2. Annual saturation indices of calcite, dolomite, montmorillonite, forsterite, lizardite, hydromagnesite, and amorphous silica in the porewaters of the control, Ol10, and Ol20 plot. Values are an average over the monitoring period of at least 3 porewater samples.

	Calcite	Dolomite	Montmorillonite	Forsterite	Lizardite	Hydromagnesite	SiO_2 (am)
Control							
2022	0.77	0.66	2.02	-9.14	-4.61	-16.1	-1.37
2023	0.96	1.10	1.7	-8.51	-3.73	-14.7	-1.47
Ol10							
2022	0.58	0.26	2.30	-9.87	-5.70	-17.3	-1.36
2023	0.82	0.70	1.90	-9.27	-5.57	-16.1	-1.47
Ol20							
2022	0.61	0.30	2.00	-9.88	-5.70	-17.3	-1.31
2023	0.83	0.83	1.34	-9.13	-4.64	-15.6	-1.44

Appendix D: Porewater chemistry

D.1 Nitrate and sulfate concentrations

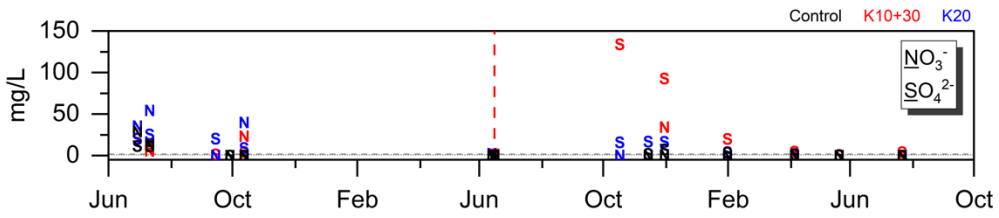

Fig. D.1. Concentrations of NO_3^- and SO_4^{2-} in porewaters in the control, K10+30, and K20 plot over three monitoring periods. Larger data gaps occur when water samples were unobtainable, e.g., during winter months. The dashed grey line indicates the average NO_3^- level (1.8 ppm) in Peterborough rainfall while the dotted grey line indicates the average SO_4^{2-} level (0.8 ppm).

D.2 Phosphorus concentrations

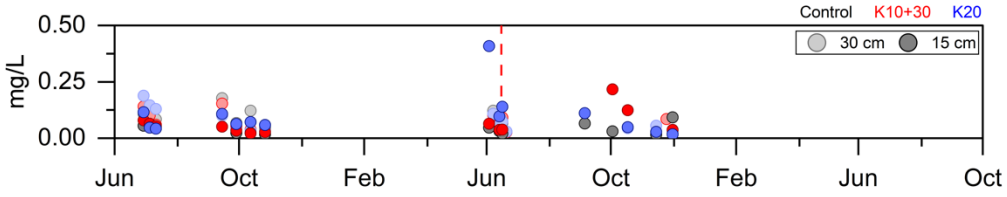

Fig. D.2. Concentrations of phosphorus in porewaters in the control, K10+30, and K20 plot over two monitoring periods. Larger data gaps occur when water samples were unobtainable, e.g., during winter months.

D.3 Nitrate and sulfate concentrations

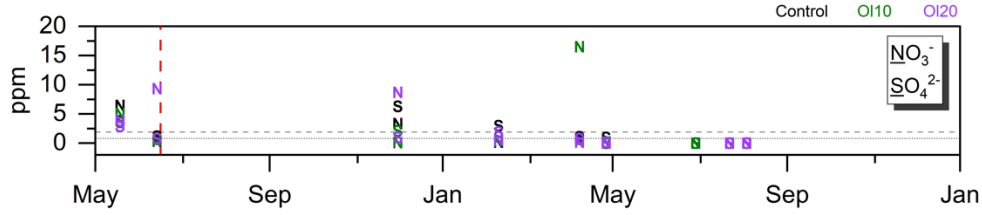

Fig. D.3. Concentrations of NO_3^- and SO_4^{2-} in porewaters in the control, Ol10, and Ol20 plot over two monitoring periods. Larger data gaps occur when water samples were unobtainable, e.g., during winter months. The dashed grey line indicates the average NO_3^- level (1.8 ppm) in Peterborough rainfall while the dotted grey line indicates the average SO_4^{2-} level (0.8 ppm).